0026-895X/92/060947-05$03.00/0

MOLECULAR PHARMACOLOGY, 42:947-951

ACCELERATED COMMUNICATION

High Affinity Block of Myocardial L-Type Calcium Channels by the Spider Toxin ω-Aga-toxin IIIA: Advantages over 1,4-Dihydropyridines

CHARLES J. COHEN, ERIC A. ERTEL, McHARDY M. SMITH, VIRGINIA J. VENEMA, MICHAEL E. ADAMS, and MARK D. LEIBOWITZ

Department of Membrane Biochemistry and Biophysics, Merck Research Laboratories, Rahway, New Jersey 07065 (C.J.C., E.A.E., M.M.S., M.D.L.), and Department of Entomology, University of California at Riverside, Riverside, California 92521 (V.J.V., M.E.A.)

Received August 26, 1992; Accepted September 11, 1992

SUMMARY

The peptide ω-agatoxin IIIA (ω-Aga-IIIA) from venom of the funnel web spider *Agelenopsis aperta* blocks L-type Ca^{2+} channels in neurons and myocardial cells with high affinity. We report that ω-Aga-IIIA also blocks whole-cell Ca^{2+} channel currents in guinea pig atrial myocytes. Although other high affinity blockers of L-type Ca^{2+} channels are available (such as the 1,4-dihydropyridines), ω-Aga-IIIA is a valuable pharmacological tool; ω-Aga-IIIA is the only known ligand that blocks L-type Ca^{2+} channels with high affinity at all voltages (IC_{50} ≈1 nM) and it causes little or no block of T-type Ca^{2+} channels, unlike the 1,4-dihydropyridines. We use ω-Aga-IIIA to selectively eliminate L-type Ca^{2+} currents and we show that felodipine blocks T-type Ca^{2+} currents. Consequently, the toxin is better than dihydropyridines for separating ionic currents through voltage-dependent Ca^{2+} channels and defining their physiological function.

Myocardial cells have predominately two populations of Ca^{2+} channels, called T-type (or low-voltage activated) and L-type (or high-voltage activated) (1). Nifedipine and related DHPs, such as felodipine, block L-type Ca^{2+} channels with high affinity in a variety of tissues (2). However, the DHPs block L-type Ca^{2+} channels with high affinity only over a limited voltage range, and this block is relatively weak if drug binding equilibrates with well polarized cells (3, 4). The high concentrations of DHPs necessary to block L-type Ca^{2+} channels at all voltages can also block T-type Ca^{2+} channels (5–9). In addition, DHPs and verapamil analogs can be high affinity blockers of the voltage sensor for calcium release from the sarcoplasmic reticulum (10). Because these commonly used Ca^{2+} channel antagonists do not selectively eliminate ionic current through L-type Ca^{2+} channels, their block of excitation-contraction coupling or stimulus-secretion coupling does not unequivocally demonstrate the involvement of calcium entry through L-type Ca^{2+} channels.

Peptide toxins that selectively block neuronal Ca^{2+} channels are known (11–14). Recent studies indicate that peptide neurotoxins isolated from venom of the funnel web spider *Agelenopsis aperta* block Ca^{2+} channels in non-neuronal cells. For example, ω-Aga-IIIA blocks L-type Ca^{2+} channels in neurons and myocardial cells (15, 16). Our studies were designed to contrast the effects of ω-Aga-IIIA with those of the DHP felodipine. We used guinea pig atrial myocytes because the components of Ca^{2+} channel current can be readily quantitated and the pharmacological properties of these currents are well documented. ω-Aga-IIIA is a more selective blocker of ionic current through L-type Ca^{2+} channels than felodipine and this toxin should be a valuable pharmacological tool. A preliminary report of part of this work has been published (16).

Materials and Methods

Whole-cell voltage-clamp measurements. Single guinea pig atrial myocytes were prepared from male Duncan-Hartley guinea pigs as described previously (9, 17). The methods used for patch voltage-clamp experiments have also been described previously (9). Briefly, cells were voltage-clamped using the whole-cell configuration of the patch-clamp technique at room temperature (20–25°) (18). Membrane current was low-pass filtered using a four-pole Bessel filter with a cut-off frequency (−3 dB, f_c) of 5 kHz and was digitized at 40 kHz, unless otherwise indicated. Linear leak and capacity currents were subtracted digitally by scaling the response to test pulses from −100 to −140 mV. Zero Ca^{2+} current was defined as the current at the holding voltage, and this level is indicated by a dashed line in figures with current

ABBREVIATIONS: DHP, 1,4-dihydropyridine; ω-Aga-IIIA, ω-agatoxin IIIA; BAPTA, 1,2-bis(2-aminophenoxy)ethane-*N*,*N*,*N*′,*N*′-tetraacetic acid; HEPES, 4-(2-hydroxyethyl)-1-piperazineethanesulfonic acid.

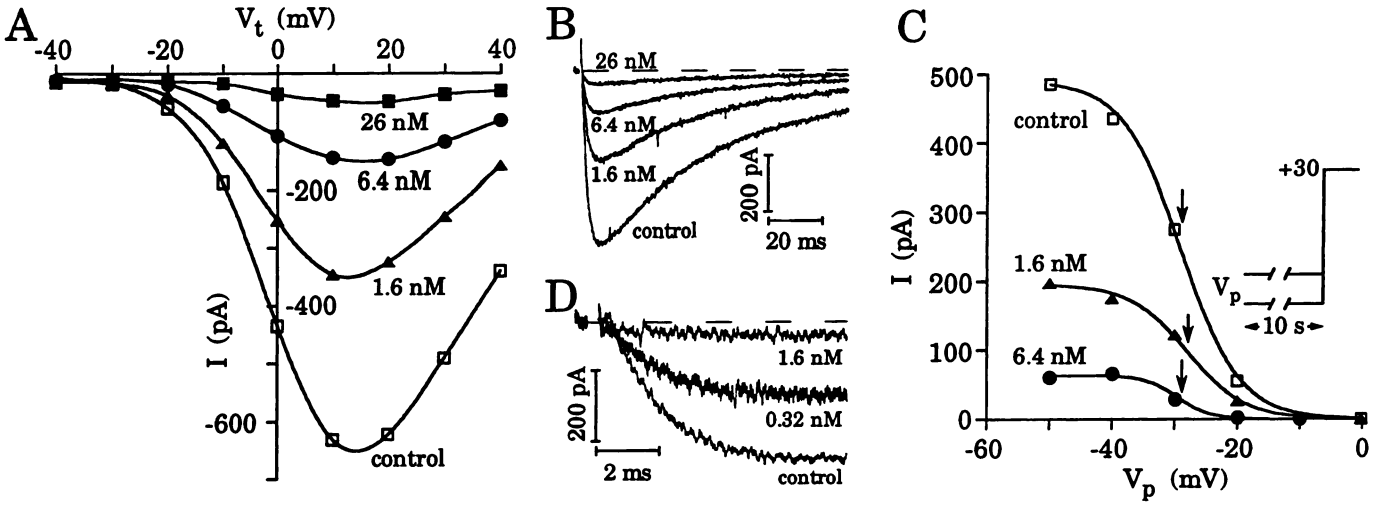

Fig. 1. High affinity voltage-independent block of L-type Ca^{2+} channels by ω-Aga-IIIA. A, Peak inward Ca^{2+} current (*I*) during 100-msec pulses to various test potentials (V_t) from a holding potential of −60 mV. □, Control; ▲, 1.6 nM; ●, 6.4 nM; ■, 26 nM ω-Aga-IIIA. The fractional block is 45%, 77%, and 92%, respectively, consistent with 1:1 binding and an IC_{50} of 2 nM. Sampling rate, 10 kHz; f_c = 2 kHz. B, Superimposed current records for V_t = +20 mV. C, Inward Ca^{2+} current at the end of a 10-msec test pulse to +30 mV versus prepulse potential (V_p). □, Control; ▲, 1.6 nM; ●, 6.4 nM ω-Aga-IIIA. *Solid curves*, fits by two-state Boltzmann distributions; *arrows*, midpoint voltages (−29.1, −28.1, and −29.5 mV). D, Superimposed current records in the low ionic strength bath solution with 0, 0.32, and 1.6 nM ω-Aga-IIIA. Holding potential, −70 mV; test potential, +5 mV; sampling rate, 50 kHz; f_c = 5 kHz.

recordings. Tail current records were fit by the sum of two exponentials plus a constant, using the Levenberg-Marquardt nonlinear curve-fitting procedure (19). Changes in membrane voltage were complete by ≈250 μsec after a change in command voltage, and data collected during this interval were excluded from analysis and display. The reported tail current amplitudes represent the magnitude of the exponentials at the end of this period. Where specified, data were fit by a two-state Boltzmann distribution $(I/I_{max} = \{1 + \exp[(V - V_{1/2})/k]\}^{-1}$, where I_{max} is the maximum amplitude, $V_{1/2}$ is the midpoint potential, and *k* is the slope factor).

Solutions and drugs. ω-Aga-IIIA was isolated from the venom of *A. aperta* by reverse phase liquid chromatography (13, 15) or by similar methodology using ion exchange and reverse phase liquid chromatography. In this venom a similar toxin, ω-Aga-$IIIA_1$, is also present.[1] It is identical to ω-Aga-IIIA except for the substitution of threonine for glutamine at residue 58. The two forms of the toxin were separated by reverse phase liquid chromatography and identified by electrospray mass spectroscopy and amino acid sequencing. Both toxins were used in our studies and their electrophysiological activities on guinea pig atrial myocytes were indistinguishable.

The external (bath) and internal (pipette) solutions for electrophysiological experiments were designed to minimize currents through Na^+ and K^+ channels and the run-down of L-type Ca^{2+} currents. Two internal solutions were used. The first (used for the experiments shown in Fig. 1) contained (in mM) cesium glutamate, 87; CsF, 20; CsCl, 20; tetrabutylammonium chloride, 1; BAPTA, 11; $CaCl_2$, 0.9; $MgCl_2$, 1; HEPES, 20; Mg-ATP, 5; and Li_2-GTP, 0.1; adjusted to pH 7.2 with CsOH. The second was identical except that CsF was replaced by equimolar cesium glutamate. The bath solution for most experiments contained (in mM) tetraethylammonium chloride, 157; $CaCl_2$, 5; $MgCl_2$, 0.5; and HEPES, 10; adjusted to pH 7.5 with CsOH; plus 0.05% fatty acid-free bovine serum albumin. The low ionic strength bath solution contained (in mM) sucrose, 267; tetraethylammonium chloride, 5; $MgCl_2$, 0.5; $CaCl_2$, 1; and HEPES, 10; adjusted to pH 7.5 with CsOH. Solutions were pressurized with 100% O_2.

Results

Current through L-type Ca^{2+} channels is commonly quantitated by measuring the peak inward current elicited during a test pulse applied from a depolarized holding potential (approximately −50 mV) (20). Such measurements show high affinity block of L-type Ca^{2+} channels by ω-Aga-IIIA (Fig. 1A). In the presence of increasing concentrations of ω-Aga-IIIA (0, 1.6, 6.4, and 26 nM), the current is reduced by the same fraction at all test potentials. Superimposed recordings of Ca^{2+} current at +20 mV with these concentrations of ω-Aga-IIIA are shown in Fig. 1B. The effect of ω-Aga-IIIA on L-type Ca^{2+} channels is similar to the effect of tetrodotoxin or saxitoxin on neuronal Na^+ channels (21); i.e., the amplitude of the current is reduced without change in time course, the fractional block is the same at all test potentials, and the concentration dependence of block is consistent with 1:1 binding to a single population of sites. In contrast, felodipine and related DHPs increase the rate of current decay during a test pulse and produce greater block at more positive test potentials (22, 23). The DHP effects are thought to reflect the voltage dependence of drug binding; the affinity between the receptor and drug is increased by channel activation or inactivation (2).

The voltage dependence of L-type Ca^{2+} channel block by DHPs is prominent when drug binding is allowed to equilibrate during long "prepulses" to various potentials. Such an experiment using ω-Aga-IIIA is shown in Fig. 1C, where the amplitude of the Ca^{2+} current at the end of a test pulse is plotted versus prepulse potential. This determines the steady state population of channels available to open for a given prepulse potential. The fractional block by ω-Aga-IIIA is the same for all potentials, indicating that block is not voltage-dependent. In contrast, DHPs and other therapeutically useful Ca^{2+} channel antagonists cause high affinity block of L-type Ca^{2+} channels only when binding equilibrates at depolarized potentials (3, 4).

ω-Aga-IIIA is a more potent blocker of L-type Ca^{2+} channels when the ionic strength and divalent cation concentration of the bath solution are reduced. Fig. 1D shows superimposed recordings of Ca^{2+} currents in the presence of ω-Aga-IIIA (0, 0.32, and 1.6 nM) made in a low-ionic strength, low-Ca^{2+} bath solution. Nearly all L-type Ca^{2+} current is blocked by 1.6 nM

[1] M. Adams, D. Hillyard, and M. Smith, unpublished observations.

ω-Aga-IIIA under these conditions, whereas only ≈50% of the current is blocked by the same concentration of toxin when the bath solution is of physiological ionic strength and contains 5 mM Ca^{2+} (Fig. 1B). Similar results were obtained in three other cells. At physiological pH, ω-Aga-IIIA is presumably a polycation with a net charge estimated to be +6 (13). The increase in potency may result from decreased surface charge screening, as is the case for charybdotoxin, another polycation (24, 25).

T-type Ca^{2+} channels inactivate when cells are held at depolarized potentials (−50 mV or more) and, therefore, contribute negligible current in the experiments of Fig. 1. However, these channels are available to open when cells are held at normal diastolic potentials (approximately −90 mV), resulting in a bimodal current-voltage relationship (Fig. 2). Previous studies with myocardial cells indicate that the low-voltage activated current is through T-type Ca^{2+} channels and the high-voltage activated current is through L-type Ca^{2+} channels (20). ω-Aga-IIIA selectively blocks the high voltage-activated component, suggesting that the toxin blocks L-type but not T-type Ca^{2+} channels (Fig. 2). This result agrees with previous work using dorsal root ganglion neurons (15).

The use of ω-Aga-IIIA allows the recording of T-type Ca^{2+} channel currents in the absence of contaminating L-type Ca^{2+} channel currents. The time courses of the toxin-sensitive and toxin-insensitive components of Ca^{2+} current are shown over a broad voltage range (Fig. 3). Each row of Fig. 3 shows the control current, the current after addition of 60 nM ω-Aga-IIIA, and the difference between these two currents, for test potentials between −40 and +60 mV. The toxin-insensitive current (Fig. 3, *center*) is due to T-type Ca^{2+} channels; it activates at more negative potentials and inactivates more rapidly than the toxin-sensitive current due to L-type Ca^{2+} channels (Fig. 3, *right*).

Tail current analysis is another way to quantitate L- and T-type Ca^{2+} currents (26). Tail currents are measured when the membrane is repolarized after a depolarizing pulse that activates channels. Their time course usually indicates the rate of channel closing (deactivation). L-type Ca^{2+} channels deactivate rapidly, whereas T-type Ca^{2+} channels deactivate slowly (9, 26). ω-Aga-IIIA at 60 nM has no effect on the slowly decaying component of tail current, confirming that T-type Ca^{2+} channels are not affected (Fig. 4A). In contrast, the current measured during the test pulse and the rapidly decaying component of tail current are substantially reduced. If the rapidly decaying tail current represents only current through L-type Ca^{2+} channels, then the fractional block is much less than expected from the potency and stoichiometry inferred from Fig. 1.

The rapidly decaying toxin-insensitive tail current probably represents asymmetric intramembrane charge movement rather than ionic current through L-type Ca^{2+} channels (Fig. 4B). In this experiment, the holding potential is −50 mV so that only L-type Ca^{2+} channels are available to open. Three current records for a test pulse to +20 mV are superimposed.

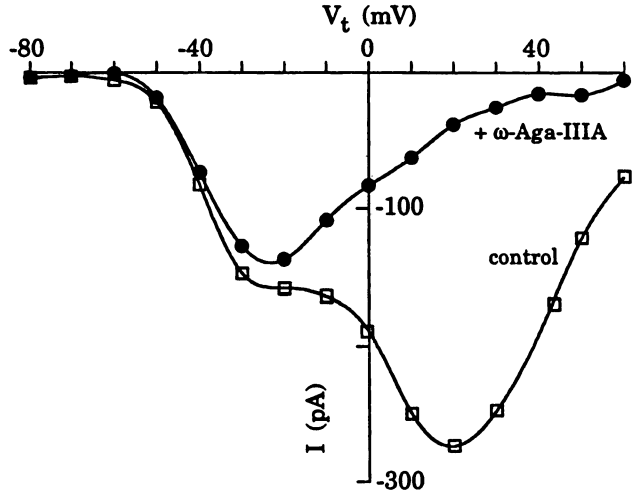

Fig. 2. ω-Aga-IIIA does not block T-type Ca^{2+} channels. Inward Ca^{2+} current (I) at the end of a 10-msec test pulse to various test potentials (V_t) from a holding potential of −90 mV. □, Control; ●, 60 nM ω-Aga-IIIA.

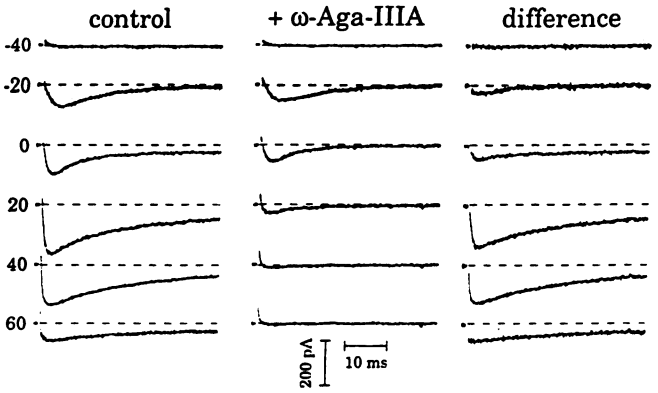

Fig. 3. Isolation of T-type Ca^{2+} currents with ω-Aga-IIIA. *Left*, control currents measured at the indicated test potential from a holding potential of −90 mV. *Center*, toxin-insensitive currents measured in 60 nM ω-Aga-IIIA. *Right*, toxin-sensitive currents obtained by subtracting the current record in toxin from the corresponding control record. Sampling rate, 10 kHz; f_c = 5 kHz.

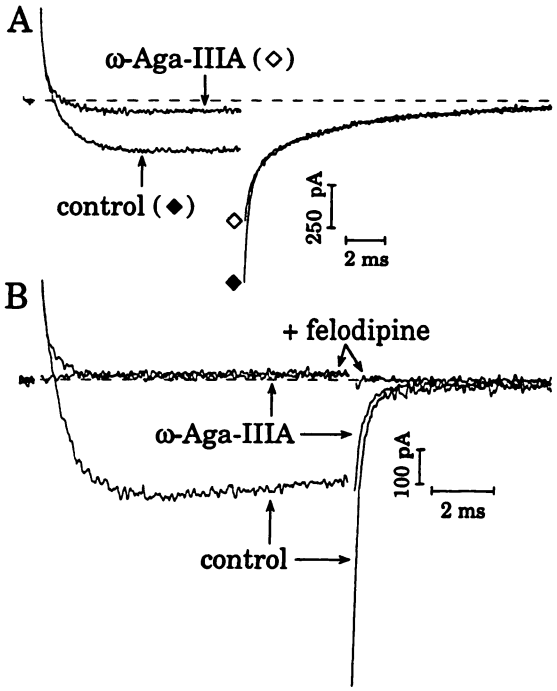

Fig. 4. Block of tail currents by ω-Aga-IIIA and felodipine. A, Superimposed current records for V_t = +20 mV from a holding potential of −90 mV in the absence (◆) and presence (◇) of 60 nM ω-Aga-IIIA (same cell as in Fig. 2). B, Superimposed current records for V_t = +20 mV from a holding potential of −50 mV for control, 60 nM ω-Aga-IIIA, and toxin plus 4 μM felodipine (different cell than in A).

The control record has three components; during the test pulse a rapidly decaying outward transient is followed by an inward current and after repolarization there is a large tail current. The record obtained in the presence of 60 nM ω-Aga-IIIA shows that this toxin has no effect on the outward transient, blocks the inward current during the test pulse (revealing a small outward current), and reduces the rapidly decaying tail current by ≈70%. The toxin-insensitive rapidly decaying tail current is present when all L-type Ca^{2+} current is blocked during the test pulse to +20 mV and is about the same size as the outward current transient at the beginning of the pulse. The subsequent addition of 4 μM felodipine blocks all remaining transient currents. DHPs are known to suppress some asymmetric charge movement in myocardial cells (27–30). These results suggest that the toxin-insensitive tail current is due to intramembrane charge movement and that ω-Aga-IIIA blocks all L-type Ca^{2+} channels with high affinity. Previous studies suggest that the DHP-sensitive charge movement represents the gating current associated with L-type Ca^{2+} channels (27–30). We have investigated this possibility in detail and will present the results elsewhere.

Felodipine blocks T-type Ca^{2+} current, whereas ω-Aga-IIIA does not (Fig. 5A). The current-voltage relationship for Ca^{2+} currents is shown under control conditions, with 10 or 50 nM ω-Aga-$IIIA_1$, and with toxin plus 1 or 5 μM felodipine. As in Fig. 2, this toxin blocks only the high-voltage activated component of Ca^{2+} current. The remaining current, which is through T-type Ca^{2+} channels, is blocked by felodipine. Similar results were obtained in seven of eight experiments.

The block of T-type Ca^{2+} channels by felodipine was confirmed by tail current analysis. The steady state availabilities of the rapidly (Fig. 5B) and slowly (Fig. 5C) decaying components of tail current were determined simultaneously. As in Fig. 4A, ω-Aga-IIIA partially blocks the rapidly decaying tail current with little or no effect on the slowly decaying tail current. Addition of 200 nM felodipine produces block of the remaining rapidly deactivating tail current, probably due to block of intramembrane charge movement. Felodipine also causes substantial voltage-dependent block of the slowly deactivating Ca^{2+} current, indicating potent block of T-type Ca^{2+} channels. The potency of this block of T-type Ca^{2+} channels by felodipine agrees with other experiments that omitted the use of ω-Aga-IIIA (9). The elimination of L-type current with ω-Aga-IIIA shows that the sensitivity of the slowly deactivating tail current to felodipine is not due to contaminating L-type Ca^{2+} current.

ω-Aga-IIIA at 120 nM had little or no effect on Na^+ currents in atrial myocytes (data not shown). High concentrations of toxin sometimes dramatically increased the holding current. It is unlikely that ω-Aga-IIIA forms channels because the toxin does not alter the conductance of lipid bilayers and does not lyse red blood cells.[2] Similar "leak" currents in atrial myocytes were sometimes caused by 1–2 mM Cd^{2+}. The origin of these leak currents remains undefined.

Discussion

ω-Aga-IIIA is a valuable tool for characterizing the pharmacology of Ca^{2+} channels in non-neuronal cells. It is the only known ligand that selectively blocks L-type Ca^{2+} channels with high affinity (IC_{50} ≈1 nM) at all voltages, without affecting T-type Ca^{2+} channels. In contrast, the DHPs only block L-type Ca^{2+} currents with high affinity when cells are subjected to maintained depolarizations (3, 4). This pattern of Ca^{2+} channel block is critical for the tissue specificity and therapeutic use of the DHPs but seriously compromises their utility as pharmacological probes for L-type Ca^{2+} channels. Furthermore, DHPs have high affinity effects on the voltage sensor that controls Ca^{2+} release from the sarcoplasmic reticulum (10). It is not possible to predict the potency of DHP block in most studies of Ca^{2+}-dependent stimulus-response coupling, and block is often so weak that secondary sites of action cannot be excluded. ω-Aga-IIIA is useful for pharmacological studies but is unlikely to be a therapeutically useful Ca^{2+} channel blocker because block of L-type channels is not voltage dependent. This toxin blocks L- and N-type Ca^{2+} channels in sensory neurons with comparable potency (15), inhibits the binding of ω-conotoxin GVIA to rat and chick brain membranes (13, 31), and blocks high K^+-induced $^{45}Ca^{2+}$ entry into chick synaptosomes (13).

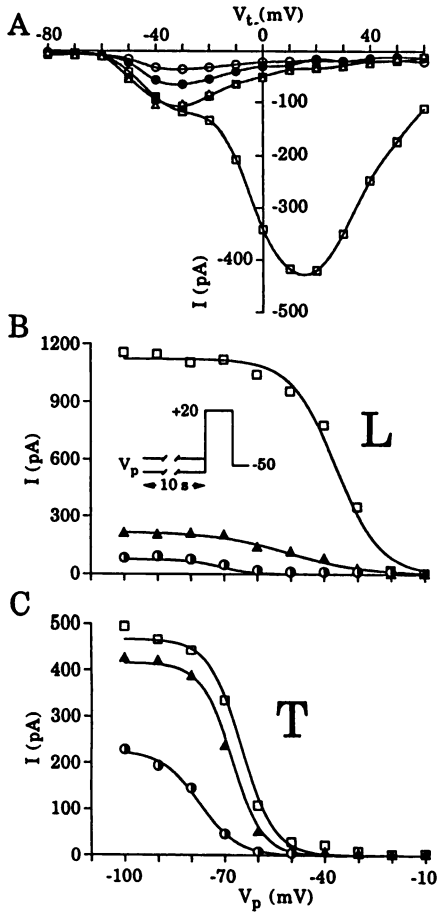

Fig. 5. Felodipine blocks T-type Ca^{2+} channel currents. A, Inward Ca^{2+} current (*I*) at the end of a 10-msec test pulse to various test potentials (V_t) from a holding potential of −90 mV. □, Control; △, 10 nM ω-Aga-IIIA; ■, 50 nM ω-Aga-IIIA; ●, toxin plus 1 μM felodipine; ○, toxin plus 5 μM felodipine. B and C, Steady state availabilities of the rapidly deactivating (B) and the slowly deactivating (C) tail current, in the same cell. □, Control; ▲, 60 nM ω-Aga-IIIA; ◑, toxin plus 200 nM felodipine. Tail currents were measured at −50 mV after a 10-msec test pulse to +20 mV from the indicated prepulse potentials. Each data set was fit by a two-state Boltzmann distribution. In B, the midpoint voltages are −35.6 mV for the control, −53.5 mV for 60 nM ω-Aga-IIIA, and −73.9 mV for toxin plus felodipine. In C, the midpoint voltages are −65.9, −68.9, and −77.5 mV, respectively.

[2] K. Giangiacomo and J. Humes, unpublished observations.

Studies with ω-Aga-IIIA, felodipine, and ω-conotoxin suggest that the classification of Ca^{2+} channels into L-, T-, N-, and P-types is oversimplified. This scheme incorrectly presumes that DHPs and ω-conotoxin are selective high affinity ligands, each specific for a single type of Ca^{2+} channel (32). For example, DHPs block several types of Ca^{2+} channels, and ω-conotoxin blocks multiple types of neuronal Ca^{2+} channels (1, 33, 34). In addition, ω-Aga-IIIA blocks both L- and N-type Ca^{2+} channels with similar affinity (15) but it does not block all ω-conotoxin-sensitive Ca^{2+} influx (13). Given these limitations, the nomenclature for Ca^{2+} channels needs to be replaced with a scheme based on the relative affinity of a series of ligands, as was required for neurotransmitter receptors. Implementation of such a scheme requires a set of high affinity probes and we believe that the family of Ca^{2+} channel toxins from funnel web spider venom can partially serve this purpose.

Acknowledgments

We thank T. Bale for excellent technical assistance and Drs. J. Arena, M. Garcia, and R. Slaughter for helpful discussions.

References

1. Bean, B. P. Classes of calcium channels in vertebrate cells. *Annu. Rev. Physiol.* **51**:367–384 (1989).
2. Janis, R. A., P. J. Silver, and D. J. Triggle. Drug action and cellular calcium regulation. *Adv. Drug Res.* **16**:309–591 (1987).
3. Bean, B. P. Nitrendipine block of cardiac calcium channels: high affinity binding to the inactivated state. *Proc. Natl. Acad. Sci. USA* **81**:6388–6392 (1984).
4. Sanguinetti, M. C., and R. S. Kass. Voltage-dependent block of calcium channel current in the calf cardiac Purkinje fiber by dihydropyridine calcium channel antagonists. *Circ. Res.* **55**:336–348 (1984).
5. Cohen, C. J., R. T. McCarthy, P. Q. Barrett, and H. Rasmussen. Ca channels in adrenal glomerulosa cells: K^+ and angiotensin II increase T-type Ca channel current. *Proc. Natl. Acad. Sci. USA* **85**:2412–2416 (1988).
6. Akaike, N., H. Kanaide, T. Kuga, M. Nakamura, J.-I. Sadoshima, and H. Tomoike. Low-voltage activated calcium current in rat aorta smooth muscle cells in primary culture. *J. Physiol. (Lond.)* **416**:141–160 (1989).
7. Kuga, T., J.-I. Sadoshima, H. Tomoike, H. Kanaide, N. Akaike, and M. Nakamura. Actions of Ca^{2+} antagonists on two types of Ca^{2+} channels in rat aorta smooth muscle cells in primary culture. *Circ. Res.* **67**:469–480 (1990).
8. Loirand, G., C. Mironneau, J. Mironneau, and P. Pacaud. Two types of calcium currents in single smooth muscle cells from rat portal vein. *J. Physiol. (Lond.)* **412**:333–349 (1989).
9. Cohen, C. J., S. Spires, and D. Van Skiver. Block of T-type Ca channels in guinea pig atrial cells by antiarrhythmic agents and calcium channel antagonists. *J. Gen. Physiol.*, **100**:703–728 (1992).
10. Rios, E., and G. Pizarro. Voltage sensor of excitation-contraction coupling in skeletal muscle. *Physiol. Rev.* **71**:849–908 (1991).
11. Gray, W. R., and B. M. Olivera. Peptide toxins from venomous *Conus* snails. *Annu. Rev. Biochem.* **57**:665–700 (1988).
12. Scott, R. H., A. C. Dolphin, V. P. Bindokas, and M. E. Adams. Inhibition of neuronal Ca^{2+} channel currents by the funnel web spider toxin ω-Aga-IA. *Mol. Pharmacol.* **38**:711–718 (1990).
13. Venema, V. J., K. M. Swiderek, T. D. Lee, G. M. Hathaway, and M. E. Adams. Antagonism of synaptosomal calcium channels by subtypes of ω-agatoxins. *J. Biol. Chem.* **267**:2610–2615 (1992).
14. Mintz, I. M., V. J. Venema, K. M. Swiderek, T. D. Lee, B. P. Bean, and M. E. Adams. P-type calcium channels blocked by the spider toxin ω-Aga-IVA. *Nature (Lond.)* **355**:827–829 (1992).
15. Mintz, I. M., V. J. Venema, M. E. Adams, and B. P. Bean. Inhibition of N- and L-type Ca^{2+} channels by the spider venom toxin ω-Aga-IIIA. *Proc. Natl. Acad. Sci. USA* **88**:6628–6631 (1991).
16. Leibowitz, M. D., T. Bale, M. E. Adams, V. J. Venema, and C. J. Cohen. Selective block of atrial L-type Ca channels by the spider toxin ω-Aga-IIIA. *Soc. Neurosci. Abstr.* **16**:956 (1990).
17. Mitra, R., and M. Morad. A uniform enzymatic method for dissociation of myocytes from hearts and stomachs of vertebrates. *Am. J. Physiol.* **249**:H1056–H1060 (1985).
18. Hamill, O. P., A. Marty, E. Neher, B. Sakmann, and F. J. Sigworth. Improved patch-clamp techniques for high-resolution current recording from cells and cell-free membrane patches. *Pflügers Arch.* **391**:85–100 (1981).
19. Press, W. H., B. P. Flannery, S. A. Teukolsky, and W. T. Vetterling. *Numerical Recipes*. Cambridge University Press, Cambridge, UK (1986).
20. Bean, B. P. Two kinds of calcium channels in canine atrial cells. *J. Gen. Physiol.* **85**:1–30 (1985).
21. Hille, B. Pharmacological modifications of the sodium channels of frog nerve. *J. Gen. Physiol.* **51**:199–219 (1968).
22. Lee, K. S., and R. W. Tsien. Mechanism of calcium channel blockade by verapamil, D600, diltiazem and nitrendipine in single dialysed heart cells. *Nature (Lond.)* **302**:790–794 (1983).
23. Aaronson, P. I., T. B. Bolton, R. J. Lang, and I. MacKenzie. Calcium currents in single isolated smooth muscle cells from the rabbit ear artery in normal-calcium and high-barium solutions. *J. Physiol. (Lond.)* **405**:57–75 (1988).
24. Vazquez, J., P. Feigenbaum, G. Katz, V. F. King, J. P. Reuben, L. Roy-Contancin, R. S. Slaughter, G. J. Kaczorowski, and M. L. Garcia. Characterization of high affinity binding sites for charybdotoxin in sarcolemmal membranes from bovine aortic smooth muscle. *J. Biol. Chem.* **264**:20902–20909 (1989).
25. Anderson, C. S., R. MacKinnon, C. Smith, and C. Miller. Charybdotoxin block of single Ca^{2+}-activated K^+ channels. *J. Gen. Physiol.* **91**:317–333 (1988).
26. Matteson, D. R., and C. M. Armstrong. Properties of two types of calcium channels in clonal pituitary cells. *J. Gen. Physiol.* **87**:161–182 (1986).
27. Shirokov, R., R. Levis, N. Shirokova, and E. Rios. Two classes of gating current from L-type Ca channels in guinea pig ventricular myocytes. *J. Gen. Physiol.* **99**:863–895 (1992).
28. Bean, B. P., and E. Rios. Nonlinear charge movement in mammalian cardiac ventricular cells. *J. Gen. Physiol.* **94**:65–93 (1989).
29. Field, A. C., C. Hill, and G. D. Lamb. Asymmetric charge movement and calcium currents in ventricular myocytes of neonatal rat. *J. Physiol. (Lond.)* **406**:277–297 (1988).
30. Hadley, R. W., and W. J. Lederer. Properties of L-type calcium channel gating current in isolated guinea pig ventricular myocytes. *J. Gen. Physiol.* **98**:265–285 (1991).
31. Ertel, E. A., C. J. Cohen, M. D. Leibowitz, M. Adams, T. Nguyen, I. M. Ashley, and M. M. Smith. Type III ω-agatoxins define similar binding sites on N- and L-type Ca channels. *Biophys. J.* **61**:419a (1992).
32. Tsien, R. W., P. T. Ellinor, and W. A. Horne. Molecular diversity of voltage-dependent Ca^{2+} channels. *Trends Pharmacol. Sci.* **12**:349–354 (1991).
33. Wang, X., S. N. Treistman, and J. R. Lemos. Two types of high-threshold calcium currents inhibited by ω-conotoxin in nerve terminals of rat neurohypophysis. *J. Physiol. (Lond.)* **445**:181–199 (1992).
34. Artalejo, C. R., R. L. Perlman, and A. P. Fox. ω-Conotoxin GVIA blocks a Ca^{2+} current in bovine chromaffin cells that is not of the "classic" N type. *Neuron* **8**:85–95 (1992).

Send reprint requests to: Charles J. Cohen, Merck Research Laboratories, P. O. Box 2000, Room 80N-31C, Rahway, NJ 07065.